Environmental Microbiome

RESEARCH

Open Access

Integrating depth-dependent protist dynamics and microbial interactions in spring succession of a freshwater reservoir

Indranil Mukherjee[1*], Vesna Grujčić[2], Michaela M. Salcher[1], Petr Znachor[1,3], Jaromír Seďa[1], Miloslav Devetter[1,4], Pavel Rychtecký[1], Karel Šimek[1,3] and Tanja Shabarova[1*]

Abstract

Background Protists are essential contributors to eukaryotic diversity and exert profound influence on carbon fluxes and energy transfer in freshwaters. Despite their significance, there is a notable gap in research on protistan dynamics, particularly in the deeper strata of temperate lakes. This study aimed to address this gap by integrating protists into the well-described spring dynamics of Římov reservoir, Czech Republic. Over a 2-month period covering transition from mixing to established stratification, we collected water samples from three reservoir depths (0.5, 10 and 30 m) with a frequency of up to three times per week. Microbial eukaryotic and prokaryotic communities were analysed using SSU rRNA gene amplicon sequencing and dominant protistan groups were enumerated by Catalysed Reporter Deposition-Fluorescence in situ Hybridization (CARD-FISH). Additionally, we collected samples for water chemistry, phyto- and zooplankton composition analyses.

Results Following the rapid changes in environmental and biotic parameters during spring, protistan and bacterial communities displayed swift transitions from a homogeneous community to distinct strata-specific communities. A prevalence of auto- and mixotrophic protists dominated by cryptophytes was associated with spring algal bloom-specialized bacteria in the epilimnion. In contrast, the meta- and hypolimnion showcased a development of a protist community dominated by putative parasitic Perkinsozoa, detritus or particle-associated ciliates, cercozoans, telonemids and excavate protists (Kinetoplastida), co-occurring with bacteria associated with lake snow.

Conclusions Our high-resolution sampling matching the typical doubling time of microbes along with the combined microscopic and molecular approach and inclusion of all main components of the microbial food web allowed us to unveil depth-specific populations' successions and interactions in a deep lentic ecosystem.

Keywords 18S and 16S amplicon sequencing, CARD-FISH, Freshwater, Microbial food webs, Protists, Epilimnion, Metalimnion, Hypolimnion, Spring succession

*Correspondence:
Indranil Mukherjee
indranilmukherjee04@yahoo.com
Tanja Shabarova
shabrik@gmail.com
Full list of author information is available at the end of the article

Background

Microbial eukaryotes, the main contributors of eukaryotic diversity on Earth, include a remarkable diversity of single-celled planktonic protists that are omnipresent across all aquatic environments. Their significance in ecosystems stems from their diverse functions in carbon fluxes and energy transfer in aquatic food webs [1, 2], encompassing a spectrum of ecological and biochemical roles and nutrition modes, from autotrophy/mixotrophy to heterotrophy (including predation, decomposition, parasitism, and osmotrophy) [3–7].

For a long time, research on protists faced limitations due to labour-intensive microscopic analyses and the often low morphological resolution of these organisms, particularly evident in the case of numerically dominant but taxonomically diverse small cells of heterotrophic nanoflagellates (HNF) [8–10]. However, the situation changed with the advent of high-throughput sequencing and the accessibility of 18S rRNA gene amplicon approaches. This transformation propelled protist research into a prominent focus within microbial ecology. Subsequently, there has been a rapid increase in studies from the early 2000s reporting an unprecedented diversity of nano-sized protists in marine [11–15] and freshwater [16–22] environments.

Most studies conducted in freshwaters have focused on the epilimnion, the upper water layer of highest productivity, while protist communities of deeper strata have been largely neglected, with only a few exceptions [21, 23–27]. Additionally, the temporal resolution of most datasets is limited to low sampling frequencies (weeks to months) that is insufficient for capturing the rapid dynamics of fast-growing protists (replicating in hours to days) [7, 28, 29]. This considerably hinders the understanding of dynamic environmental events such as phytoplankton spring blooms [30, 31] or impacts of dramatic environmental disturbances [32]. In temperate freshwater lakes, the onset of spring is marked by a physical mixing event after ice melt, which uniformly distributes microbial populations in the water column. The increase of light intensity and air temperature leads to a thermal stratification of the water column and rapid growth of phototrophic organisms in the epilimnion that serve as a base for the aquatic food web. The succession of phytoplankton and zooplankton during this phase was well described in the original and revised Plankton Ecology Group (PEG) model [33, 34]. Recently, an attempt was made to expand the PEG model to encompass seasonal dynamics of prokaryotes [35]. The detailed resolution of bacterial spring dynamics showed a dominance of fast-growing phytoplankton bloom-associated Bacteroidota and Gammaproteobacteria at the beginning of spring bloom [30, 31, 36, 37], succeeded by small-sized Actinobacteriota that are generally more resistant to protistan grazing [30, 38]. However, our understanding of bacterial dynamics in the hypolimnion during this seasonal event remains limited [31]. While the revised PEG model includes protistan abundance [34], and protists have been documented in various prokaryotic studies to estimate top-down control, the broader scope of bacterial-protist interactions beyond prey-grazer dynamics remains unexplored. Additionally, there is still a lack of information regarding the spring succession of individual protistan populations, their ecological associations, and their functions within the aquatic food web across distinct lake strata [39].

Shotgun metagenomic analyses which successfully resolve bacterial populations by providing metagenome assembled genomes of high quality, have an unfortunate constraint for research on protist communities. This is due to a small number of sequenced protist genomes available in public databases and the increase in computational power and necessary depth of sequencing which grows exponentially with the increase in cell and genome size of sequenced organisms [31]. Therefore, many studies introduce arbitrary cutoffs of 20 or 5 µm for filtration and thus do not provide information on larger protists as well as symbiotic interactions, which might be crucial during the springtime [33, 34].

In this study conducted in the temperate freshwater Římov reservoir (Czech Republic), we used a cutoff of 200 µm for biomass collection and hybrid approach combining 18S rRNA gene amplicon sequencing with the fluorescent labelling technique Catalysed Reporter Deposition-Fluorescence in situ Hybridization (CARD–FISH) [6, 22, 24, 40, 41]. This allowed us to visualise and enumerate specific protistan lineages, which dominated the sequencing data [39, 42]. Additionally, we analyzed 16S rRNA gene amplicons of the prokaryotic community, phyto- and zooplankton, viruses, and chemical parameters, aiming at identifying dominant protist populations and their major interactions to refine our comprehension of the spring plankton succession in different strata of the reservoir. We hypothesised that protist communities in the hypolimnion significantly differ from those found in upper water layers. Specifically, we expected that variations in prey availability and the prevalence of attached lifestyle will strongly influence protist dynamics, ultimately leading to distinct microbial community interactions within the hypolimnion.

Methods

Study site and sampling procedure

The Římov reservoir, situated in South Bohemia, Czech Republic, is a dimictic, meso-eutrophic canyon-shaped reservoir which serves as an important drinking water

supply. It covers an area of 2.06 km^2 with a volume of 34.5×10^6 m^3 and an average summer retention time of 77 days. It has been studied since 1979 at well–established stations [43], one of them located in the lacustrine zone near the dam (48.8475817N, 14.4902242E, max. depth 43 m) was used for sampling in our study.

Sampling was conducted during the period 31st March to 25th May 2016, with the high-frequency sampling, i.e. three times per week, conducted between 7 April to 12 May over the most intensive part of the spring bloom phase (for the detailed description of the sampling dates and hydrological parameters see Additional file 1). We sampled 3 depths (0.5, 10 and 30 m), which corresponded to the epi-, meta-, and hypolimnion, respectively. The sampling started during the mixing period (at homogeneous temperature distribution in the water column) covered the establishment of stratification and was terminated with the end of clear-water phase recognized by increased chlorophyll *a* concentrations. The samples were taken with a Friedinger sampler (Šramhauser; spol.s.r.o., Dolní Bukovsko, Czech Republic). For each depth ten litres of water were prefiltered through a 200 µm mesh plankton net into a plastic barrel which was precleaned with household bleach and rinsed with Milli-Q and sample water. Physical and chemical parameters, i.e., water temperature, pH, dissolved oxygen, and oxygen saturation were measured with a multiparametric probe YSI EXO2 (Yellow Springs Instruments, Yellow Springs, OH, USA). A submersible fluorescence probe (FluoroProbe; bbe-Moldaence, Kiel, Germany) was employed to measure chlorophyll *a* (Chl-*a*) concentrations at 0.2 m intervals down till 20 m depth. Water transparency was measured using a Secchi disc. Samples for chemical analysis were collected in separate bottles. Phytoplankton samples were collected from 0.5 m depth and preserved with a Lugol's solution for further processing. Crustacean zooplankton was sampled once a week by vertical hauls using an Apstein plankton net (200-um mesh). Net hauling provided an integrated sample for the upper 5 m water column representing the epilimnetic layer. Two hauls were combined into one sample and preserved with formaldehyde (4% final concentration) for subsequent processing in the laboratory. Small-sized rotifers were sampled analogically once a week as an integrated sample from the upper 5 m water column using a plastic tube of the appropriate length. Subsequently, a volume of 40 l of collected water was quantitatively filtered using a 35 µm thickening net. The collected material was preserved with formaldehyde (4% final concentration).

Chemical analysis

Samples were analysed for pH, dissolved organic carbon (DOC), dissolved nitrogen (DN), dissolved silica (DSi), total phosphorus (TP), dissolved phosphorus (DP), dissolved reactive phosphorus (DRP), NH_4-N, NO3-N and absorbance was measured at wavelengths 254, 300, 350 and 400 nm (Additional file 2) using methods summarized in Znachor et al. [43].

Enumeration of microbial cells, viruses, phytoplankton and zooplankton

For each depth, subsamples were fixed with the Lugol-formaldehyde-thiosulfate decolourization technique (2% final concentration of formaldehyde) to minimize ejection of protistan food vacuole contents [44]. These samples were used for the enumeration of bacteria on black 0.2 µm pore-size filters (Osmonics, Inc., Livermore, CA, USA) and eukaryotes (flagellates and ciliates) on black 1 µm pore-size filters. All samples were stained with DAPI (4′, 6-diamidino-2-phenylindole, 1 µg ml^{-1} final concentration) and microbes were counted via epifluorescence microscopy (Olympus BX 53; Optical Co., Tokyo, Japan). For enumeration of virus-like particles (VLP), subsamples were fixed with glutaraldehyde (1% final concentration) for 10 min, flush-frozen with liquid nitrogen and stored at -80 °C until further processing. VLP were counted with an inFlux V-GS cell sorter (Becton Dickinson, Franklin Lakes, NJ. USA) as previously described [45].

Phytoplankton species were enumerated employing the Utermöhl method with an inverted microscope (Olympus IX 71) [46]. The mean dimension of algal cells were obtained for biovolume calculation using the approximation of cell morphology to regular geometric shapes [47].

For the analysis of zooplankton, formaldehyde from the preserved material was removed and partially replaced by tap water. Further processing was performed by a classical microscopical counting of different species with a series of species determination keys [48]. Rotifer abundance was analysed in exact subsamples in counting chamber using dissecting microscope Leica DM 2500 under magnification of 25–40×. Species determination was done according to Koste 1978 [49] in light of more recent literature in particular families and recent taxonomy.

DNA extraction and sequencing

Prokaryotic and eukaryotic biomass was collected on 0.2 µm pore-size filters (47 mm diameter; Osmonics, Minnetonka, MN, USA) from 1500 to 2000 ml of water. DNA was extracted with the Power Water DNA isolation kit (MO BIO Laboratories, Inc, Carlsbad, CA, USA). Prokaryotic 16S rRNA fragments (V4 region) were amplified using primer pair 515F and 926R [50] and sequenced on an Illumina MiSeq platform (PE300) with V3 chemistry at Genome Research Core of the University

of Illinois (Chicago, USA). Eukaryotic amplicons (V9 region) were prepared using Euk_1391F and EukBr-7R primers (https://earthmicrobiome.org/protocols-and-standards/18s/) and sequenced on an Illumina MiSeq platform (PE250) with V2 chemistry at SEQme company (Dobříš, Czech Republic).

Sequence analysis

Primers were cut from the demultiplexed reads using Cutadapt software v2.8 [51]. Trimmed sequences were processed using DADA2 pipeline v1.16.0 [52] with standard parameters (https://benjjneb.github.io/dada2/tutorial.html) in R (R Core Team 2020). For taxonomic identification at ASV (Amplicon Sequence Variant) level, SILVA v138 [53, 54] and PR^2 v4.14.0 [55] were used for prokaryotes and eukaryotes, respectively. All irrelevant reads (mitochondria and plastids for prokaryotes and metazoa and fungi for eukaryotes as the study was focussed on protists) and singletons were excluded, and both datasets were rarefied to the smallest read number prior diversity estimation and statistical analysis. In order to access relatedness of microbial communities of different lake strata and their temporal dynamics, a Bray–Curtis dissimilarity distance matrices were calculated for protists and prokaryotes. Based on the obtained matrices, we performed nonparametric multidimensional scaling (nMDS) analysis using XLSTAT14 (Addinsoft, USA). Diversity estimators and indexes were calculated using vegan package in R [56]. A co-occurrence network was used to find associations between common protistan and prokaryotic ASVs (relative abundances > 0.5% in at least one sample). Subsequently, all possible pairwise Spearman's rank correlations were calculated with the R script https://github.com/RichieJu520/Co-occurrence_Network_Analysis [57]. Only robust ($|r| > 0.7$) and statistically significant ($p < 0.05$) correlations were visualized in Gephi v0.9.2 [58] with subsequent modular analysis. The sequence data generated from amplicon sequencing were submitted to the European Nucleotide Archive (ENA) and are available under the BioProject: PRJEB66298.

Phylogenetic tree reconstruction, design of novel eukaryotic probes, and catalysed reporter deposition fluorescence in situ hybridization (CARD-FISH)

Representative amplicons of the 30 most abundant protistan ASVs were aligned with the SINA aligner [59] and imported into ARB [60] using the SILVA database SSURef_NR99_123 [61]. Alignments were manually refined and a maximum likelihood tree (1000 bootstraps) including their closest relatives was constructed on a dedicated web server [62] (Additional files 3–5). Oligonucleotide probes targeting a small, monophyletic lineage of katablepharids (Kat2-651), Telonema (Telo-1250) and Novel Clade 10 of Cercozoa (NC10–1290) were designed in ARB using the tools probe_design and probe_check and evaluated with the web tool math-FISH [63]. The formamide percentages were optimized on environmental samples (Table 1, Additional file 6).

CARD-FISH was carried out for eight protistan lineages (Table 1) following published protocols [39]. Hybridized cells were visualized with an Olympus BX 53 epifluorescence microscope under 1000 × magnification at blue/UV excitations.

Estimation of bacterivory rates of HNF and ciliates

Flagellate and ciliate bacterivory rates in the epilimnion were estimated using fluorescently labelled bacteria (FLB) [64], prepared from a mixture of strains from the genus *Limnohabitans* and *Polynucleobacter* [65]. Briefly, the FLB tracers were added to constitute 8–20% of total bacteria. Samples were incubated at in situ temperature with FLB tracers for 5 and 30 min for ciliate and flagellate grazing rates, respectively. Incubation was terminated by fixation with Lugol-formaldehyde-thiosulfate and DAPI stained subsamples were prepared as described above for microscopical analysis [65, 66]. A minimum of 100

Table 1 CARD-FISH probes used in the study

Probe name	Target	Sequence 5′–3′	Formamide concentration (%)	References
Crypto B	Cryptophyceae	ACGGCCCCAACTGTCCCT	50	[101]
Cry1-652	CRY1 lineage of cryptophytes	TTTCACAGTWAACGATCCGCGC	30	[40]
Kat-1452	Katablepharidacea	TTCCCGCARMATCGACGGCG	60	[40]
Kat2-651	Katablepharidacea clade 2	GACCRYYTGTCAAACTCCAAAATCCAA	50	This study
Kin516 EUK516	Kinetoplastea Competitor	ACCAGACTTGTCCTCC ACCAGACTTGCCCTCC	30	[102]
Perkin01	Perkinsozoa clade 1	GAGGATGCCTCGGTCAA	30	[103]
Telo-1250	Telonemia	CAGYCAAGGTGGACAACTYGTT	40	This study
NC10-1290	Cercozoa novel clade 10	CTAGCCCCATCRCGTTGCGA	40	This study

ciliates and 200 HNF were inspected for FLB ingestion in each sample. To estimate total protistan grazing, average bacterial uptake rates of ciliates and HNF were multiplied by their in situ abundances.

Results

Physical and chemical parameters and abundance of microbes

The temperature profile from the first sampling date (31st March 2016) indicated an almost homogeneously mixed water column with only two degrees difference between the surface and the bottom (Fig. 1a). Similarly, the concentration of dissolved oxygen was almost uniform between 10 to 12 mg l^{-1} in the entire water column (Fig. 1b). At the end of the sampling campaign (25th May), when the water column was stratified, the epilimnion temperature reached 16.6 °C, with a thermocline established between 5–10 m depth. Soon after the beginning of the sampling campaign, hypoxia started to develop in the bottom layers, which became anoxic towards the end, however, the sampling depth of hypolimnion (30 m) was always oxygenated (> 6.9 mg l^{-1}; Fig. 1b). A Chl-*a* maximum (19.6 µg l^{-1}) was observed in the epilimnion in the first week of sampling after which the concentration dropped and remained relatively low till the end of the study (Fig. 1c).

Ciliates increased in the first 2 weeks to maximum abundance of 60 ind. ml^{-1} (Fig. 1d), and were dominated by prostomes i.e., *Urotricha* spp. and *Balanion planctonicum,* representing efficient hunters of small algae and flagellates [67]. Ciliate abundances dropped sharply during the clear water phase and recovered simultaneously with Chl-*a* concentrations at the study end (Fig. 1c). Low counts of HNF, prokaryotes and VLP, were recorded at the start of the sampling (Fig. 1e–g). During the first 2 weeks, the numbers of HNF increased in all water strata, with a maximum of 7.7×10^3 cells ml^{-1} in the epilimnion and lower peaks in deeper layers (4.2×10^3 and 2.9×10^3 cells ml^{-1} at 10 m and 30 m, respectively; Fig. 1e). Thereafter, the abundances gradually decreased in all layers with some occasional peaks. Bacterial abundances reached maxima in the epilimnion in mid-April (5.3×10^6 cells ml^{-1}), whereas numbers remained low in the metalimnion and hypolimnion (averaging 2.6×10^6 cells ml^{-1} and 2.0×10^6 cells ml^{-1}, respectively) (Fig. 1f). VLP steadily increased at 0.5 m to 5.6×10^7 VLP ml^{-1} and plateaued towards the end, while abundances at 10 and 30 m remained relatively stable with maxima of 3.8×10^7 VLP ml^{-1} at 10 m and 3.9×10^7 VLP ml^{-1} at 30 m (Fig. 1g).

Phytoplankton biovolume in the epilimnion peaked with 3.6 mm^{-3} l^{-1} in the first week of April, showed a sharp decline within the following two weeks and remained low until the end (Fig. 2a). Cryptophytes (*Cryptomonas reflexa, Rhodomonas minuta*) dominated the phytoplankton throughout the sampling period together with diatoms (*Cyclotella* sp., *Fragilaria sp.*) and chrysophytes (*Chrysococcus* sp.). Rotifers and cladocerans followed the phytoplankton dynamics and showed maxima in the second week of sampling (Fig. 2b). Copepod numbers increased slowly, but their populations remained stable in the second part of the study when densities of rotifers and cladocerans decreased.

Grazing impact of HNF and ciliates on bacteria

On average, HNF and ciliates grazed 0.32×10^6 bacteria day^{-1}, corresponding to 8.2% of bacterial standing stock in the epilimnion of the reservoir. HNF were the major bacterivores responsible for 73% of total protistan bacterivory, while ciliates grazing was more important at the beginning and end of the campaign (Additional file 7), coinciding with relatively low numbers of Cladocerans (Fig. 2b).

Community composition of microbes in the water column

From 51 DNA samples, 47 and 43 were successfully amplified and sequenced for prokaryotic and eukaryotic analyses, respectively. Datasets were rarefied to 31,011 (prokaryotes) and 13,202 (protists) reads per sample (Additional file 8). Both taxonomic entities displayed similar temporal developments based on their ASV dynamics. After mixing, we observed a fast separation of epilimnion samples from the deeper lake strata and undirected fluctuations and delayed differentiation of meta- and hypolimnetic communities (Fig. 3). Reduction of diversity over the time was noticed in both prokaryotes and protists especially in the epilimnion (Fig. 3). Despite similar dynamic patterns observed at highly resolved taxonomic level, prokaryotes showed more unified composition at family to phylum levels than protists (Fig. 4a). Specifically, Actinobacteriota, Verrucomicrobiota, Chloroflexota and several families of Gammaproteobacteria (Comamonadaceae, Burkholderiaceae and Methylophilaceae) were distributed at comparable relative abundances in all samples from all layers. In contrast, among protists only Katablepharida and Ciliophora showed comparable distributions (Fig. 4b, Additional file 9).

The epilimnion was characterised by a high contribution of Bacteroidota (max. 35%) and increasing read counts of Alphaproteobacteria (max. 26%) and Armatimonadota (max. 3%) towards the study end (Fig. 4a). The eukaryotic community was dominated by cryptophytes with the highest ASV contribution of 70% on 18th April (Fig. 4b). Synurophytes also contributed a significant number of reads, especially towards the study end (up

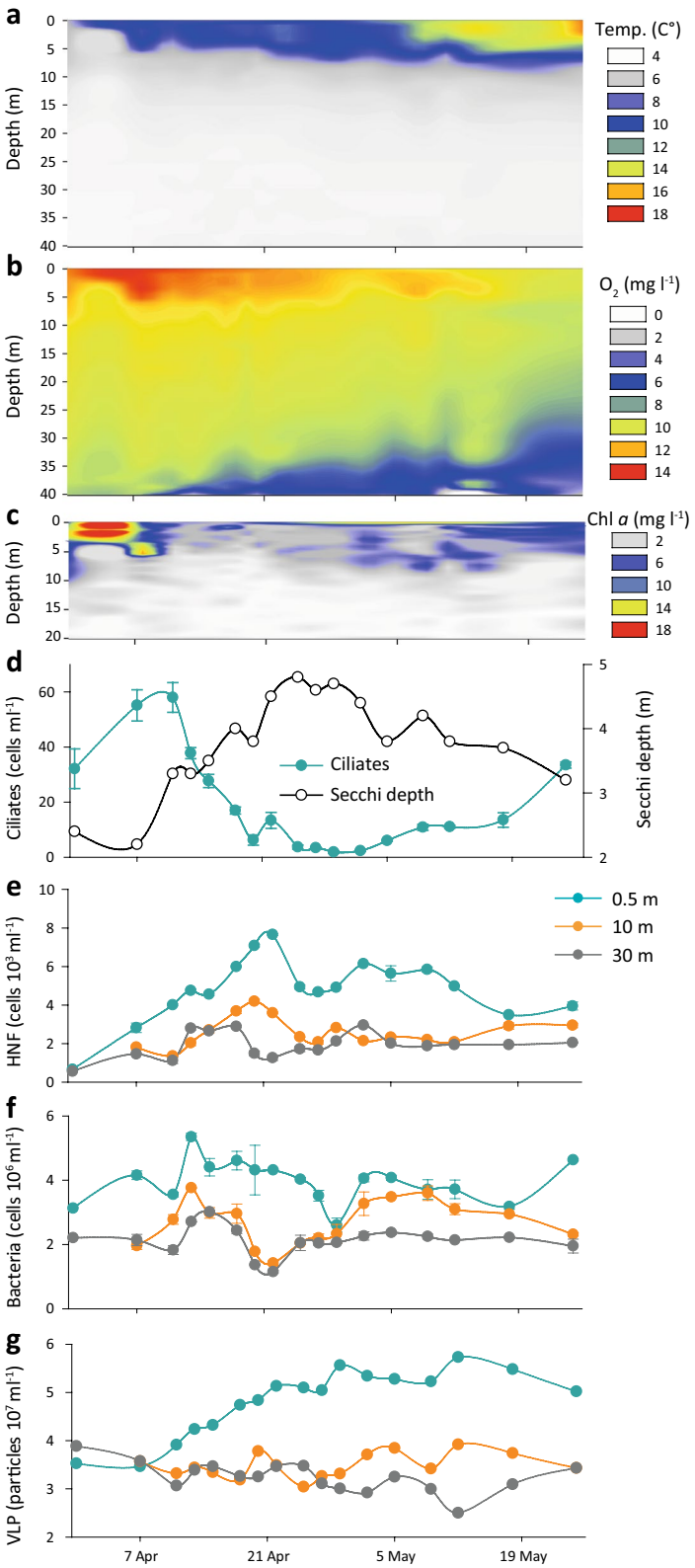

Fig. 1 Main physical and chemical parameters and abundances of microorganisms observed in the Římov reservoir during the study. **a** Thermal structure of the water column (Temp). **b** Vertical distribution of oxygen (O_2). **c** Chlorophyll *a* profile (0–20 m). **d** Abundances of ciliates in the epilimnion and Secchi depths. **e** Abundances of heterotrophic nanoflagellates (HNF) at three depths. **f** Bacterial abundances at three depths. **g** Abundances of virus like particles (VLP) at three depths

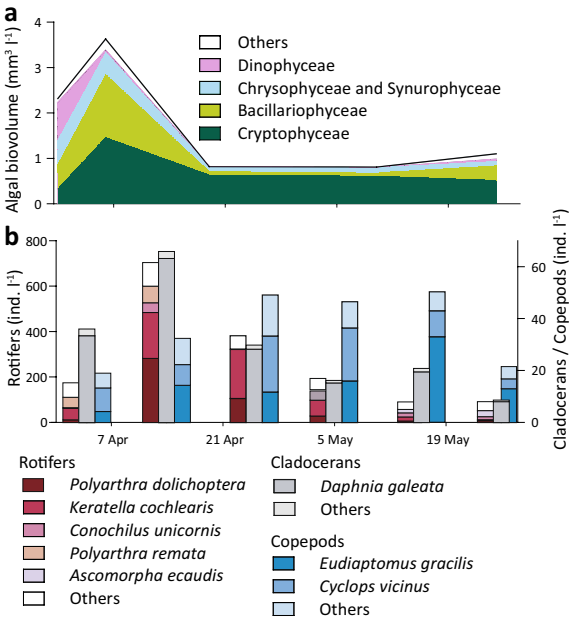

Fig. 2 Phytoplankton biovolume (**a**) and zooplankton abundance (**b**) in the epilimnion of Římov reservoir during the study

to 30%). Apicomplexa, almost absent at the beginning, increased in relative abundances as the study progressed and reached 10% on 25th April.

Among prokaryotes in the metalimnion, a high proportion of Planctomycetota was present throughout the study period, in contrast to negligible counts in the upper water layer. Moreover, populations of Acidobacteriota, Gallionellaceae, Nitrosomonadaceae, Legionellaceae and TRA3-20 established in the metalimnion albeit at low percentages (Fig. 4a, Additional file 8). Similar to the epilimnion, cryptophytes were the most dominant eukaryotic group and represented up to 40% on 25th April and 5th May (Fig. 4b). In contrast, Dinophyta, Chrysophyta, Cercozoa, Telonema and Excavata had significantly higher contributions to the metalimnetic community (Additional file 8).

In the hypolimnion, we observed a collapse of Bacteroidota population after 25th April, the date corresponding to the breakpoint clearly separating the meta- from hypolimnion according to nMDS analysis (Fig. 3). While the majority of bacterial groups were common to both metalimnetic and hypolimnetic samples (Fig. 4a), Methylomonadaceae and Solimonadaceae were present exclusively in the hypolimnion. The eukaryotic community in the hypolimnion was dominated by Perkinsozoan sequences (max. 30%), especially towards the study end (Fig. 4b). Similar to Bacteroidota, cryptophyte sequences drastically dropped after 25th April which reflected the separation of hypolimnion from the metalimnion (Figs. 3, 4b). Chrysophytes had a relatively high contribution in the hypolimnion during the early phase of the campaign but dropped considerably towards the study end. Cercozoa, Telonemia and Dinophyta had relatively high and stable proportions throughout the campaign.

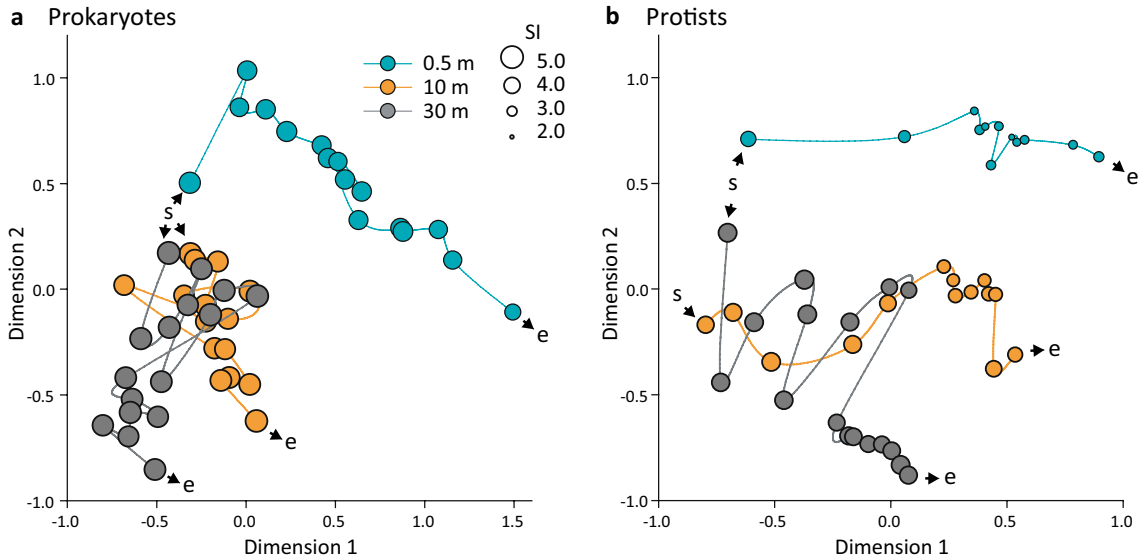

Fig. 3 Nonparametric multidimensional scaling plots reflecting dynamics of prokaryotic (**a**) and protistan (**b**) communities at three depths of Římov reservoir. Plots are based on Bray–Curtis's distance matrices calculated on rarefied ASV datasets. Kruskal's stress values are 0.096 and 0.079 for prokaryotic and protistan plots respectively. The sampling start is indicated with the letter 's', and the end is indicated with the letter 'e'. The lines are connecting communities according to the temporal course of the study. Diameters of the circles correspond to the Shannon–Wiener diversity index (SI)

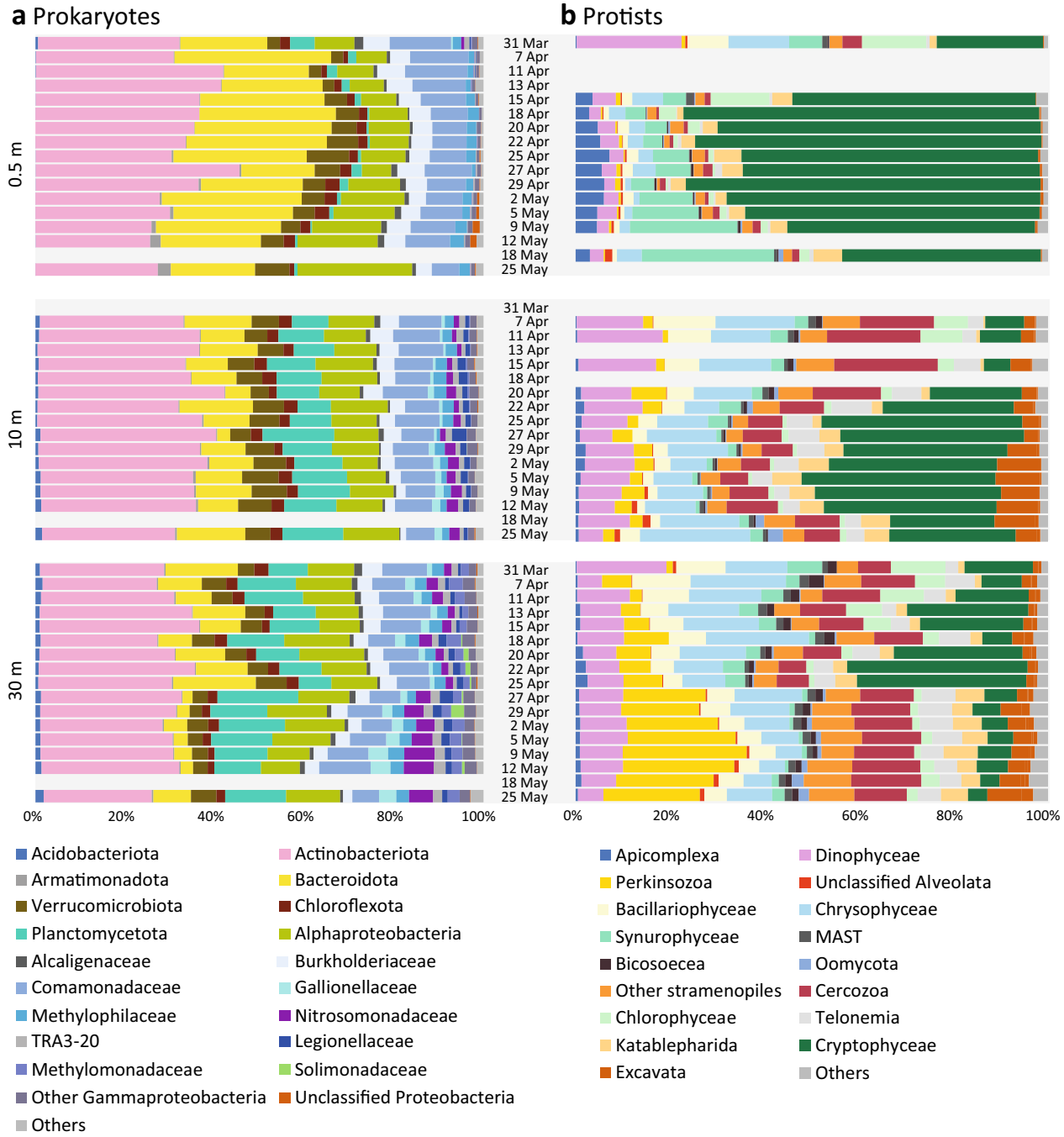

Fig. 4 Prokaryotic and protistan community composition at three depths of Římov reservoir during the study. The gaps indicate missing samples. **a** Prokaryotic community. The majority of groups are resolved at phylum to class levels, with the exception of Gammaproteobacteria where several families were shown due to high heterogeneity in their distribution. **b** Protistian community. The groups are resolved at phylum to class level, with the exception of Supergroup Excavata, which was dominated by kinetoplastea. Ciliophora were excluded from the analysis of protists due to homogeneous distribution with high proportions in all the three layers. The figure including ciliophora is available in Additional file 9

Dynamics of important groups of microbial eukaryotes in the water column

Cell abundances of eight eukaryotic groups were quantified by CARD-FISH using specific probes (Table 1, Fig. 5, Additional files 9, 10). Cryptophytes dominated in the epilimnion for about three weeks from late April to early May (max. 4.3×10^3 cells ml^{-1}) and decreased towards the study end. Their abundances

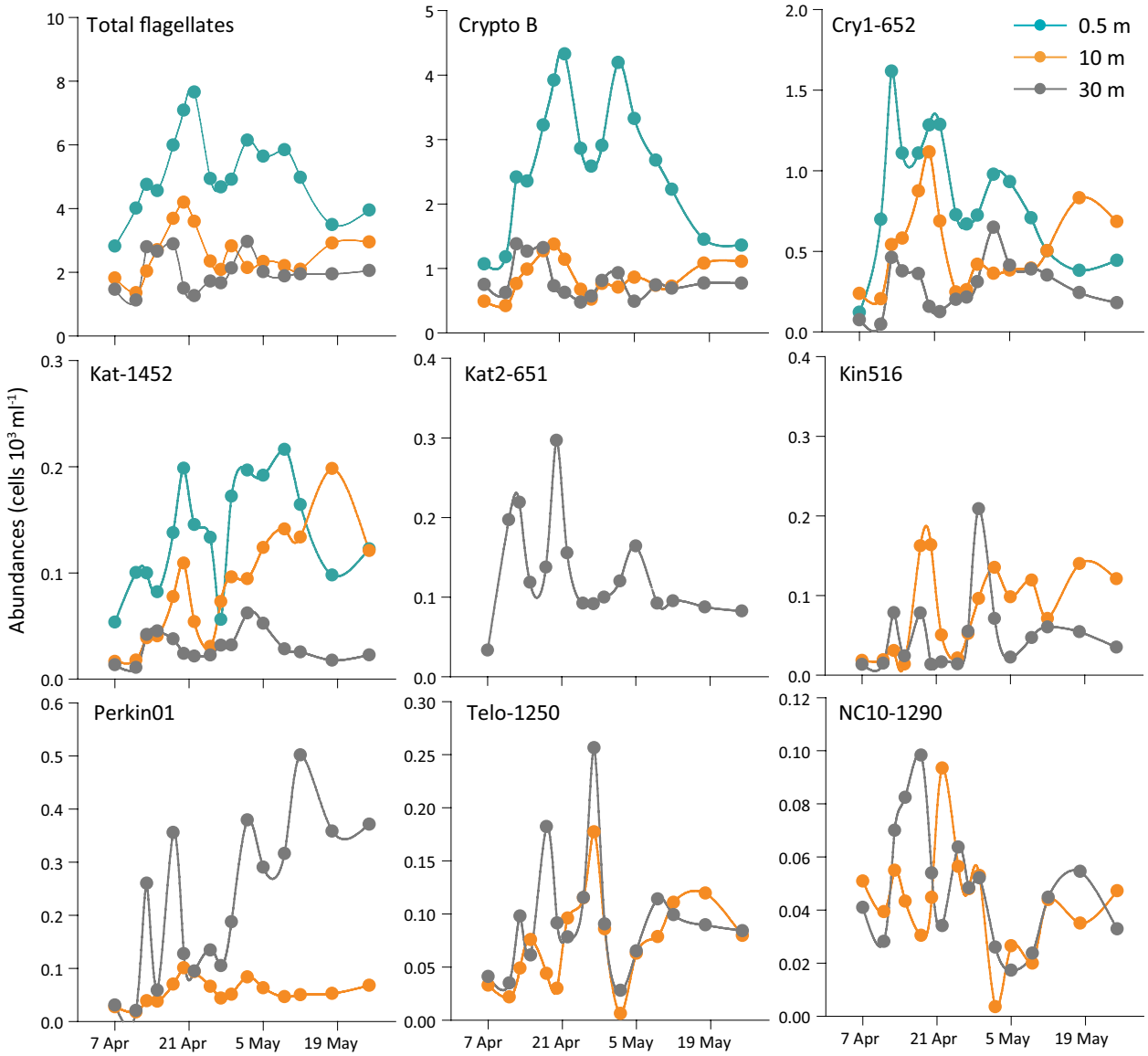

Fig. 5 Absolute abundances of particular flagellate groups at three depths of Římov reservoir obtained by CARD-FISH. Left to right from top-total eukaryotes by DAPI staining, cryptophytes targeted by probe Crypto B, CRY1 lineage of cryptophytes targeted by probe Cry1-652, katablepharids targeted by probe Kat-1452, katablepharid clade 2 targeted by probe Kat2-651, kinetoplastids targeted by probe Kin516, Perkinsozoa clade 1 targeted by probe Perkin01, Telonemids targeted by probe Telo-1250, and Cercozoa Novel Clade 10 targeted by probe NC10-1290. A figure representing relative abundances of flagellates can be found in the supplemental material (Additional file 10)

in the meta- and hypolimnion remained relatively low ($<1.4\times10^3$ cells ml^{-1}). Epilimnetic abundances of the aplastidic CRY1 lineage of cryptophytes initially increased to 1.6×10^3 cells ml^{-1} (34% of the total eukaryotes) on April 13th (Fig. 5, Additional file 10) and decreased to 0.4×10^3 cells ml^{-1} towards the study end. In the metalimnion, abundances of this lineage showed similar but less pronounced dynamics and reached maxima on 20th April with 1.1×10^3 cells ml^{-1} (27% of total eukaryotes). Their abundance in the hypolimnion was relatively low ($<0.6\times10^3$ cells ml^{-1}, $<22\%$ of total eukaryotes).

Katablepharids targeted by probe Kat-1492 were not abundant in the epilimnion with exception of two peaks of ca. 0.2×10^3 cells ml^{-1} (Fig. 5). In the metalimnion, their abundance gradually increased and represented up to 7% of total eukaryotes (Additional file 10). In the hypolimnion, this lineage showed low numbers throughout the study period, in contrast to the katablepharids detected with probe Kat2-651 which

were found exclusively in the hypolimnion with up to 0.3×10^3 cells ml^{-1} (Fig. 5).

Kinetoplastida, Perkinsozoa, Telonema and Cercozoa Novel Clade 10 were detected only in the meta- and hypolimnion (Fig. 5). In the metalimnion, Kinetoplastida increased with some oscillations till the study end with maxima of 0.18×10^3 cells ml^{-1}. Similarly, their abundances fluctuated considerably with maxima of 0.21×10^3 cells ml^{-1} in the hypolimnion. Perkinsozoans targeted by probe Perkin01 had relatively low abundances in the metalimnion (max. 0.1×10^3 cells ml^{-1}), while they reached up to 0.5×10^3 cells ml^{-1} in the hypolimnion (Fig. 5). Telonema were abundant in meta- and hypolimnion samples with the highest peaks recorded on 25th April with 0.17×10^3 cells ml^{-1} and 0.26×10^3 cells ml^{-1}, respectively. The Novel Clade 10 of Cercozoa showed similar abundance patterns to those observed for Telonema (Fig. 5). However, maximal abundances were two–three times lower, i.e., 0.09×10^3 cells ml^{-1} and 0.10×10^3 cells ml^{-1} in meta- and hypolimnion, respectively.

Microbial interactions in different water layers

We performed a network analysis to examine the connections between and within the eukaryotic and bacterial communities (Fig. 6). The majority of potential interactions were located in two large clusters consisting of three modules each. The modules of the smaller cluster reflected the temporal development within the epilimnion. Phototrophic eukaryotes, such as *Cryptomonas* (Cryptophyta), *Chlamydomonas* (Chlorophyta) and Chrysophyta had central positions and were excessively linked to Flavobacteriales, Chitinophagales and Sphingobacteriales, which contributed the highest proportion of nodes in this cluster (Fig. 6, Additional file 11). Ciliates within the epilimnetic network cluster, such as *Vorticella* sp., were associated with colonial chrysophytes,

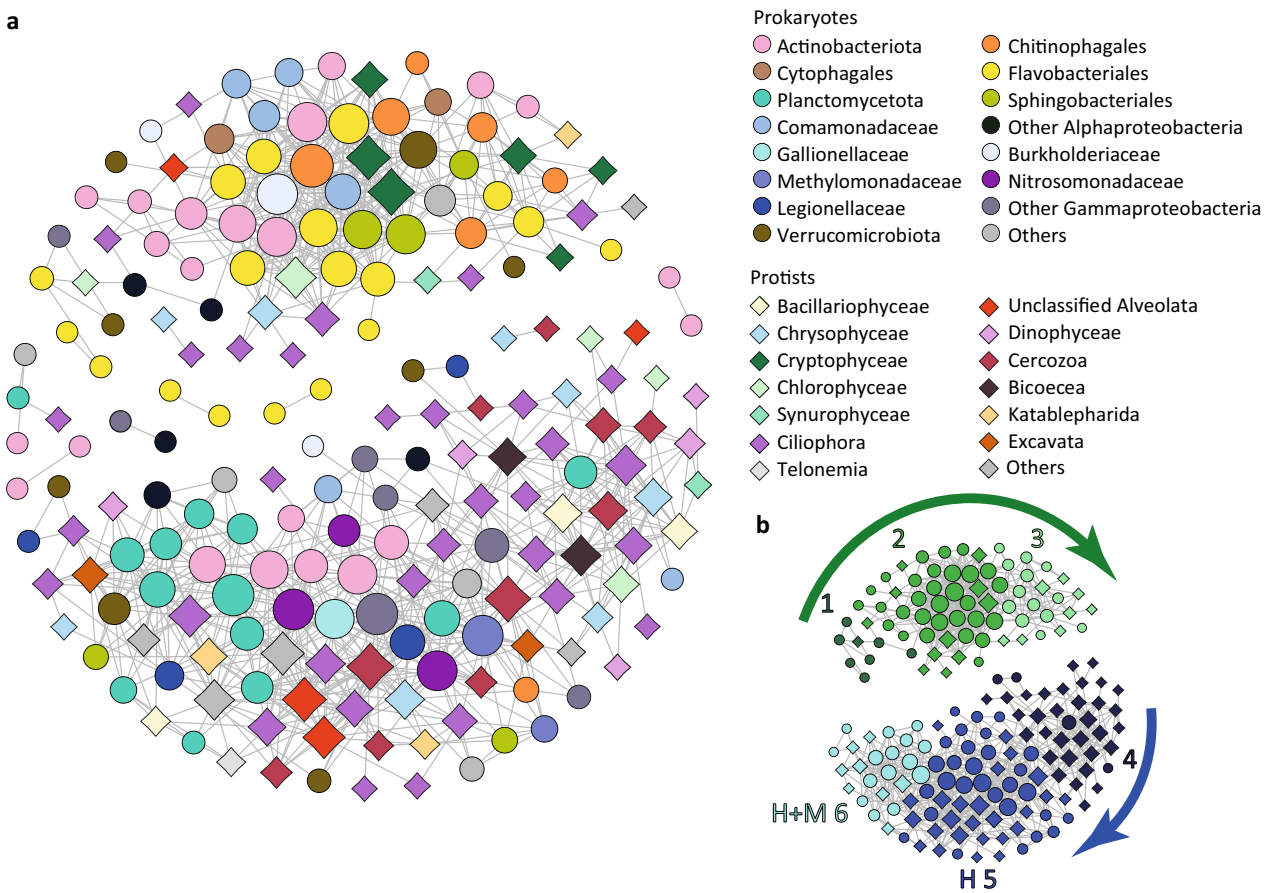

Fig. 6 Network analysis based on the most abundant ASVs from protistan and prokaryotic communities. **a** Network: upper cluster represents the community dominating in the epilimnion, lower cluster represents the community dominating in the hypolimnion. Prokaryotic nodes are displayed as circles, protistan nodes as diamonds. **b** The main modules detected in the network. The arrows indicate directions of temporal shifts between modules. Differentiation between modules H 5 and H + M 6 is based on spatial parameters as module 6 was also well represented by members of the metalimnion community

while *Rimostrombidium* and *Strombidium* spp., exhibited extensive connections to bacterial nodes. The modules in the large meta- and hypolimnion associated cluster showed a limited temporal resolution. The module four represented the earliest part of the sampling period and consisted mainly of protists affiliated to Bicosoecida, Cercozoa and Ciliophora organized around centric diatoms (Fig. 6, Additional file 11). Heterotrophic flagellated protists Bicosoecea and Cercozoa along with Ciliophora (*Vorticella, Tokophrya, Tintinnidium* etc.) comprised the lion share of this module. Chrysophytes and dinophytes were additional microbial eukaryotic groups detected in module four. A highly interconnected bacterial node in this part of the network was affiliated with Pirellulaceae (Planctomycetota) and was linked to diatoms, bacterivorous cercozoans and ciliates. Interestingly, four *Legionella* spp. ASVs were part of the hypolimnion network and were linked to eukaryotes. Moreover, in two cases, this was a selective connection to single eukaryotic ASVs (a ciliate and a cercozoan) and a simultaneous association with Verrucomicrobiota (Fig. 6, Additional file 11). Rather than showing a temporal distinction, modules five and six exhibited a depth-related separation (Fig. 6, Additional file 11). Module five was more aligned with the hypolimnion, while module six represented the community interactions in both meta- and hypolimnion. Similar to module four, the microbial eukaryotes present in module five were mainly excavates and cercozoans. Excavates such as kinetoplastids represented two nodes in the network modules five and also module six (Fig. 6, Additional file 11). One additional node in module five was represented by the predatory protist group Telonema. Planctomycetota prevalent in module six were mainly represented by members of Nemodikiaceae (CL500-3 group). Ammonia oxidizers such as Nitrosomonadaceae were also present in this module and were connected to nitrite oxidizers, e.g. *Nitrotoga* sp. (Gallionellaceae) and ASVs affiliated with *Methylobacter*.

Discussion

High-frequency sampling, reflecting the typical doubling time of microbes, allowed us to follow tightly the community assembly at three depths during the transition from mixis to stratification in the water column. Interestingly, both protistan and prokaryotic community development showed strikingly similar dynamics in the different water strata of the reservoir (Fig. 3). The eukaryotic and bacterial communities in the epilimnion gradually diverged from those in the meta- and hypolimnion soon after the mixing, responding to the increase in temperature and light intensity. Moreover, towards the end of the campaign when the water column became stratified, we observed a clear separation between meta- and hypolimnetic communities.

Formation of water strata-associated communities and detected microbial interactions

The network analysis allowed us to follow the interaction between prokaryotes and protists and to shed light on their potential ecological and trophic roles in the epilimnion and hypolimnion of Římov reservoir (Fig. 6). Phototrophic eukaryotes found in the epilimnion cluster were the typical recurrently appearing members of spring blooms [34]. They were associated with Flavobacteriales, Chitinophagales and Sphingobacteriales known to be efficient decomposers of phytoplankton derived exudates and polymers during spring blooms [31, 36, 37] (Fig. 6, Additional file 11). In the later phase of the study the protists exhibited increased connections with bacteria known as potential consumers of small molecular substances such as *Polynucleobacter* sp., Actinobacteriota and copiotrophic Comamonadaceae. These bacterial groups are well recognized members of spring bloom and disturbance successions [30–32, 38]. Ciliates in this cluster were mainly represented by omnivorous and moderately efficient bacterial grazers such as *Rimostrombidium* and *Strombidimum* spp. [65], linked to bacterial nodes. Their presence was also confirmed microscopically, where they contributed substantially to high ciliate numbers and grazing rates at the beginning and the end of the study (Fig. 1d, Additional file 7). Additionally, substrate attached ciliates, e.g. *Vorticella* sp. [68, 69] were found in this part of the network associated to colonial chrysophytes.

The sessile or particle-attached lifestyle was even more pronounced in the large hypolimnion cluster. Modules five and six (Fig. 6, Additional file 11) appear to be associated with lake snow (macroscopic organic aggregates or detritus particles) [70], while the module four was characterised by association between centric diatoms, which were probably sedimenting through the water column, with *Vorticella* sp., *Tokophrya* sp. and Bicosoecida (Fig. 2a). The latter are characterized as mainly attached flagellates feeding on bacteria or more rarely free-living and feeding on particle-associated bacteria [8, 71]. Planctomycetota were a dominant bacterial phylum in the hypolimnion cluster. Specifically, in module four they were represented by Pirellulaceae, particle attached bacteria previously detected in the hypolimnion of Římov reservoir during algal blooms [72]. On the other hand, the group CL500-3, prevalent in modules five and six is also recognised for its psychrophilic nature and particle-attached lifestyle [72, 73]. These bacteria are capable of peptide degradation through the so-called 'planctosome' complex bound to the outer membrane [72, 74]. Their

activity might create micro-environments rich in labile amino acids [75] and ammonia beneficial for free-living Nanopelagicales (Actinobacteriota), specialists in the uptake of amino acids [38, 76], dominant in module five. The extensive connection between Nitrosomonadaceae (ammonia oxidizers) and Gallionellaceae (nitrite oxidizers) in the same module indicates their combined potential of nitrate production in the deep waters. Nitrate produced by these bacteria was shown to positively influence the methane oxidation efficiency of *Methylobacter* spp. (Methylomonadaceae) [77]. Cercozoans detected in different modules within the hypolimnion cluster [16, 23] were reported as feeders of bacteria and small eukaryotes [7, 78] or phytoplankton parasites [23, 79]. Both strategies corroborate the associations detected in the co-occurrence network (Fig. 6). Another putative parasitic relationship previously described in the literature [80, 81] was detected between *Legionella* sp. and eukaryotic ASVs (Fig. 6, Additional file 11).

Different feeding strategies could be responsible for lineage-specific distribution of protists in the water column, as one lineage of katablepharids (Kat2-651) was detected with CARD-FISH exclusively in the hypolimnion, while another lineage was abundant in the epi- and metalimnion (Fig. 5). Omnivorous and predatory strains of katablepharids are described in the literature [7, 41, 82]. Excavates (Kinetoplastea and Diplonemea) are typically found in the hypolimnion of freshwater lakes during summer [22, 24, 83], or in hypertrophic, shallow lakes rich in suspended organic particles [41]. In our study, the presence of kinetoplastids in the metalimnion and hypolimnion was confirmed by both sequencing and CARD-FISH data (Figs. 4, 5) in line with reports of kinetoplastids feeding on bacteria associated with detritus particles [8, 84] sinking from the epilimnion to deeper strata at the end of the spring bloom [83]. The presence of Telonema in this module also corroborated with reports from a wide range of freshwater habitats [18, 20, 24, 85]. However, our study is the first to track their population dynamics using a specific oligonucleotide probe (Table 1, Additional file 6), revealing that telonemids are almost absent in surface waters and mainly inhabit the cold deep-water layers (Figs. 4, 5).

Dynamics of dominant protistan groups

Cryptophyta was the most abundant eukaryotic group dominating in all epi- and metalimnion samples, commonly detected by both sequencing and CARD-FISH methods (Figs. 4, 5, Additional files 9, 10). Microscopic observations showed the high abundances of big (10–30 µm long) chloroplast-bearing but also small aplastidic cryptophytes. Highly abundant heterotrophic CRY1 lineage [7, 41] accounted on average for 30% of the total cryptophytes targeted by the general Crypto B probe (Fig. 5). This lineage did not show clear associations within the network but contributed substantially to the first maximum of HNF observed in epi- and metalimnion and probably played an important role as bacterivores in line with recent findings of high bacterial uptake rates of CRY1 [41, 42]. The balance between auto- and heterotrophic cryptophytes during the springtime is related to the availability of ample sunlight, nutrients and prokaryotic prey [30, 42, 86].

Perkinsozoa dominated the deep-water communities (Figs. 4, 5) and were not present in the co-occurrence network. Perkinsozoa comprise putative parasitic protists widely distributed in marine and freshwaters [21, 23, 87–89]. In our study, the contribution of Perkinsozoan ASVs and cell abundance increased with the onset of stratification (Figs. 4, 5), reaching up to 25% of total ASVs and 26% of total eukaryotes in the hypolimnion, similar to previous studies [21, 23, 31]. With CARD-FISH analysis, perkinsozoans were observed both free-living and inside of free-living protists (Additional file 6). An additional taxon well represented in the sequencing data and absent in the network analysis was Apicomplexa, a poorly understood group especially in freshwater environments. Apicomplexa were reported as obligate intracellular parasites mainly affecting fish and phytoplankton [90]. In our data set, they were more abundant in the epilimnion and significantly correlated with cryptophytes ($r^2 = 0.600$, $p = 2.719 \times 10^{-10}$). Apicomplexa and perkinsozoa were not part of the network probably due to their putative parasitic association with higher eukaryotes that were not included in analyses.

Microbial food web organization in spring

Algal blooms are the major factors shaping the spring microbial community not only in the epilimnion [91, 92] but also in the deeper strata, due to the enhanced particle flux from the surface waters [83, 93]. For an overview of the microbial food web in the Římov reservoir during spring, please see a schematic diagram (Additional file 12). The bloom of chrysophytes, diatoms and large cryptophytes in the reservoir at the beginning of the sampling campaign was likely decimated by zooplankton or viral lysis [31]. However, ciliates dominated by raptorial prostomes such as *Urotricha* spp. and *Balanion planctonicum* might also considerably contribute to the phytoplankton reduction [67, 94] (Fig. 1d). Cladocerans, especially large sized *Daphnia* spp. were highly abundant during the first 2 weeks of sampling and seemed to represent the main driver responsible for the decline of phytoplankton bloom in mid-April. The highest abundances of smaller grazers, i.e. Rotifera were observed close to the maxima of their corresponding favourite prey, i.e.

chrysophytes and cryptophytes (Fig. 2). *Polyarthra* spp., which were shown to selectively feed on chrysophytes [95], were first in the succession and were followed by omnivorous *Keratella* sp. preferably feeding on chrysophytes and cryptophytes [96]. However, *Cyclops vicinus* seemed to drastically reduce the rotifer population, similar to previous observations of spring plankton succession in Římov reservoir [97]. The simultaneous establishment of a stable population of *Eudiaptomus gracilis* probably did not contribute much to the rotifers' top-down control, but this copepod successfully replaced rotifers and daphnids as a powerful algal grazer in the later phase [98]. *E. gracilis* was also shown to exhibit strong influence on the lower food web organization due to a high clearance rate of ciliates [99]. The drop in ciliate densities, including high proportions of bacterivorous or omnivorous species, most likely resulted in a short-term increase in bacterial numbers (Fig. 1d, f). Notably, ciliates were almost equally important bacterivores as HNF during the times of high ciliate abundances (Additional file 7). Ciliates, especially raptorial prostomes also contributed to the reduction of HNF in the epilimnion (Fig. 1d, e). In addition, approximately half of the ciliate community during its peak abundance in early April was composed of typical flagellate hunters such as *Balanion planctonicum* and *Urotricha* spp. (data not shown) [7, 94, 100]. After the drop of ciliate abundance, the protistan bulk bacterivory rate was largely attributed to HNF (Additional file 7) dominated by aplastidic cryptophytes such as CRY1 lineage [41, 42] and omnivorous katablepharids (Fig. 5) [7, 41].

Communities in the deeper strata showed a clear dominance of heterotrophic groups although we did not follow the dynamics of higher trophic levels due to their low abundances. However, the highly complex network between prokaryotes and protists in the hypolimnion (Fig. 6) indicates a considerable increase of bacterivorous, parasitic, and detritivorous strategies in these strata.

Conclusions

In this study, we followed the dynamics of organisms < 200 µm in three different water column layers of a freshwater reservoir at high-temporal resolution during spring. The results unveiled parallel community assembly patterns for protists and prokaryotes, revealing an early separation of epilimnetic communities and subsequent differentiation between the meta- and hypolimnetic layers. Besides confirming a prevalence of phototrophic and predatory strategies among epilimnetic protists, we observed the emergence of organisms affiliated with Perkinsozoa, Telonemia, Kinetoplastida, and Cercozoa in the meta- and hypolimnion, indicating a dominance of particle-associated lifestyles and parasitic and detritivorous strategies in deeper strata during the spring period. Furthermore, we showcased diverse associations between bacterial and protistan taxa, ranging from substrate degradation-related to parasitic. These associations followed temporal successions and displayed depth-specific dynamics. Sequence-based and microscopic techniques allowed for the integration of protists into a holistic picture of the complex community dynamics during springtime. Such a hybrid approach appears to be a powerful tool for integrating various groups of organisms in temporal and spatial dynamics, enhancing our comprehension of microbial interactions and the functioning of freshwater ecosystems.

Supplementary Information

The online version contains supplementary material available at https://doi.org/10.1186/s40793-024-00574-5.

Additional file 1: Hydrological data and sampling dates. Precipitation data and flow rates of reservoir were provided by the Water Authority of Vltava River (Povodí Vltavy).

Additional file 2: Chemistry data. *DOC* Dissolved organic carbon, *DN* Dissolved nitrogen, *DSi* Dissolved silica, *TP* Total phosphorus, *DP* Dissolved phosphorus, DRP Dissolved reactive phosphorus, A254-400 absorbance measured at corresponding wavelength (nm).

Additional file 3: Randomized axelerated maximum likelihood (RAxML) tree (100 bootstraps) of katablepharids. Branches with bootstrap support < 20% were multifurcated, probe targets are marked by different colors. Asterisks indicate sequences not targeted by probes.

Additional file 4: Randomized axelerated maximum likelihood (RAxML) tree (100 bootstraps) of Cercozoa including Novel Clade 10 (NC10). Branches with bootstrap support < 20% were multifurcated, probe targets are marked by different colors. Asterisks indicate sequences not targeted by probe.

Additional file 5: Randomized axelerated maximum likelihood (RAxML) tree (100 bootstraps) of Telonema. Branches with bootstrap support < 20% were multifurcated, probe targets are marked by different colors. Asterisks indicate sequences not targeted by the probes, # indicates sequence that is too short to be checked for the target region.

Additional file 6: Microphotographs displaying: **a** different lineages of protists hybridized with CARD-FISH probes designed for this study (Kat2-651, Telo-1250 and NC10-1290), cell hybridized with Kat-1452 shown for comparison; **b** different lifestyles observed for Perkinsozoa hybridized with Perkin01 (upper row free-living, lower row protist-associated). The scale bar applies for all images. Microphotographs were produced using Zeiss Imager Z2, Carl Zeiss, Oberkochen, DE equipped with a Colibri LED system and the following filter sets: DAPI 49 (Excitation 365; Beamsplitter TFT 395; Emission BP 445/50), fluorescein 38 HE (Excitation BP 470/40; Beamsplitter TFT 495; Emission BP 525/50).

Additional file 7: Total grazing by protists in the epilimnion.

Additional file 8: Table of all eukaryotic and prokaryotic ASVs. Read numbers of ASVs in all samples of rarefied datasets.

Additional file 9: Protistan community composition at three depths of Římov reservoir during the study. The gaps indicate missing samples. The groups are resolved at phylum to class level, with the exception of Supergroup Excavata, which was dominated by kinetoplastea.

Additional file 10: Relative abundances of particular flagellate groups in three depths of Římov reservoir obtained with CARD-FISH analysis. Left to right from top- cryptophytes targeted with Crypto B probe, CRY1 lineage of cryptophytes targeted with Cry1-652 probe, katablepharids targeted with Kat-1452 probe, katablepharid clade 2 targeted with Kat2-651 probe,

kinetoplastids targeted with Kin516 probe, Perkinsozoa clade 1 targeted with Perkin01 probe, Telonemids targeted with Telo-1250 probe, and Cercozoa novel clade 10 targeted with NC10-1290 probe.

Additional file 11: Network analysis based on the most abundant ASVs from protistan and prokaryotic communities. **a** Network: upper cluster represents the community dominating in the epilimnion, lower cluster represents the community dominating in the hypolimnion. Prokaryotic nodes are displayed as circles, protistan nodes as diamonds. **b** The main modules detected in the network. The arrows indicate directions of temporal shifts between modules. Differentiation between modules H 5 and H+M 6 is based on spatial parameters as members of module 6 were better resented in the metalimnion communities. Prokaryotic and protistan nodes are organized into modules and listed below, accompanied by heatmaps based on Z scores calculated for each module. Samples are grouped according to water column layers, with the time course depicted from left to right.

Additional file 12: Schematic figure of food web in Římov reservoir during the studied spring period. Arrows indicate the direction of carbon flow. *DOM* Dissolved organic matter, *POM* Particulate organic matter, HNF Heterotrophic nanoflagellates.

Acknowledgements
We are thankful to Radka Malá for excellent laboratory assistance.

Author contributions
IM, VG and KŠ conceived the study. IM and TS wrote the manuscript with the input from all authors. IM performed CARD-FISH, data analysis and interpretation. VG performed sampling, CARD-FISH and data analysis. TS performed sampling, sequence data analysis and interpretation, and design of figures. MS performed sampling, phylogenetic analyses and construction of CARD-FISH probes. KŠ performed microscopic counts, bacterivory rates estimation, data analysis and interpretation. PZ, PR, JS and MD performed sampling and sample analysis. All the authors contributed to critical revisions and approved the final version of the manuscript.

Funding
This study was supported by the research Grant 22-35826 K (Grant Agency of the Czech Republic) awarded to IM, which covered all the materials and the salaries of IM and KŠ. MMS was supported by the research Grant 20-12496X (Grant Agency of the Czech Republic). TS and PZ were supported by the research Grants 23-05081S and 22-33245S, respectively. The funding bodies had no role in study design, data collection and analysis, interpretation of data or preparation of the manuscript.

Availability of data and materials
The sequence data generated from the 16S and 18S rRNA gene amplicon sequencing was submitted to the European Nucleotide Archive (ENA) and are available under the BioProject: PRJEB66298, [https://www.ebi.ac.uk/ena/browser/view/PRJEB66298].

Declarations

Ethics approval and consent to participate
Not applicable.

Consent for publication
Not applicable.

Competing interests
The authors declare that they have no competing interests.

Author details
[1]Biology Centre of the Czech Academy of Sciences, Institute of Hydrobiology, Na Sádkách 7, 37005 Ceske Budejovice, Czech Republic. [2]Department of Ecology, Environment and Plant Sciences, Stockholm University, Stockholm, Sweden. [3]Faculty of Science, University of South Bohemia, 37005 Ceske Budejovice, Czech Republic. [4]Biology Centre of the Czech Academy of Sciences, Institute of Soil Biology and Biogeochemistry, Na Sádkách 7, 37005 Ceske Budejovice, Czech Republic.

Received: 22 December 2023 Accepted: 30 April 2024
Published online: 08 May 2024

References

1. Worden AZ, Follows MJ, Giovannoni SJ, Wilken S, Zimmerman AE, Keeling PJ. Environmental science. Rethinking the marine carbon cycle: factoring in the multifarious lifestyles of microbes. Science. 2015;347:1257594.
2. Caron DA, Countway PD, Jones AC, Kim DY, Schnetzer A. Marine protistan diversity. Ann Rev Mar Sci. 2012;4:467–93.
3. Arndt H, Dietrich D, Auer B, Cleven E-J, Grafenhan T, Weitere M, Mylnikov AP. Functional diversity of heterotrophic flagellates in aquatic ecosystems. Syst Assoc Spec. 2000;59:240–68.
4. Zubkov MV, Tarran GA. High bacterivory by the smallest phytoplankton in the North Atlantic Ocean. Nature. 2008;455:224–6.
5. Caron DA, Hu SK. Are we overestimating protistan diversity in nature? Trends Microbiol. 2019;27:197–205.
6. Piwosz K. Weekly dynamics of abundance and size structure of specific nanophytoplankton lineages in coastal waters (Baltic Sea). Limnol Oceanogr. 2019;64:2172–86.
7. Simek K, Grujcic V, Mukherjee I, Kasalicky V, Nedoma J, Posch T, Mehrshad M, Salcher MM. Cascading effects in freshwater microbial food webs by predatory Cercozoa, Katablepharidacea and ciliates feeding on aplastidic bacterivorous cryptophytes. FEMS Microbiol Ecol. 2020;96:fiaa121.
8. Boenigk J, Arndt H. Bacterivory by heterotrophic flagellates: community structure and feeding strategies. Antonie Van Leeuwenhoek. 2002;81:465–80.
9. Massana R, Terrado R, Forn I, Lovejoy C, Pedros-Alio C. Distribution and abundance of uncultured heterotrophic flagellates in the world oceans. Environ Microbiol. 2006;8:1515–22.
10. Obiol A, Muhovic I, Massana R. Oceanic heterotrophic flagellates are dominated by a few widespread taxa. Limnol Oceanogr. 2021;66:4240–53.
11. Lopez-Garcia P, Rodriguez-Valera F, Pedros-Alio C, Moreira D. Unexpected diversity of small eukaryotes in deep-sea Antarctic plankton. Nature. 2001;409:603–7.
12. Moon-van der Staay SY, De Wachter R, Vaulot D. Oceanic 18S rDNA sequences from picoplankton reveal unsuspected eukaryotic diversity. Nature. 2001;409:607–10.
13. de Vargas C, Audic S, Henry N, Decelle J, Mahe F, Logares R, Lara E, Berney C, Le Bescot N, Probert I, et al. Ocean plankton. Eukaryotic plankton diversity in the sunlit ocean. Science. 2015;348:1261605.
14. Pasulka A, Hu SK, Countway PD, Coyne KJ, Cary SC, Heidelberg KB, Caron DA. SSU-rRNA gene sequencing survey of benthic microbial eukaryotes from Guaymas basin hydrothermal vent. J Eukaryot Microbiol. 2019;66:637–53.
15. Giner CR, Pernice MC, Balague V, Duarte CM, Gasol JM, Logares R, Massana R. Marked changes in diversity and relative activity of picoeukaryotes with depth in the world ocean. ISME J. 2020;14:437–49.
16. Lepere C, Boucher D, Jardillier L, Domaizon I, Debroas D. Succession and regulation factors of small eukaryote community composition in a lacustrine ecosystem (Lake Pavin). Appl Environ Microbiol. 2006;72:2971–81.
17. Grossmann L, Jensen M, Heider D, Jost S, Glucksman E, Hartikainen H, Mahamdallie SS, Gardner M, Hoffmann D, Bass D, Boenigk J. Protistan community analysis: key findings of a large-scale molecular sampling. ISME J. 2016;10:2269–79.
18. Simon M, Lopez-Garcia P, Deschamps P, Moreira D, Restoux G, Bertolino P, Jardillier L. Marked seasonality and high spatial variability of protist communities in shallow freshwater systems. ISME J. 2015;9:1941–53.
19. Simon M, Lopez-Garcia P, Deschamps P, Restoux G, Bertolino P, Moreira D, Jardillier L. Resilience of freshwater communities of small microbial eukaryotes undergoing severe drought events. Front Microbiol. 2016;7:812.

20. Khomich M, Kauserud H, Logares R, Rasconi S, Andersen T. Planktonic protistan communities in lakes along a large-scale environmental gradient. FEMS Microbiol Ecol. 2017;93:fiw231.
21. Mukherjee I, Hodoki Y, Nakano S. Seasonal dynamics of heterotrophic and plastidic protists in the water column of Lake Biwa, Japan. Aquat Microb Ecol. 2017;80:123–37.
22. Mukherjee I, Salcher MM, Andrei AS, Kavagutti VS, Shabarova T, Grujcic V, Haber M, Layoun P, Hodoki Y, Nakano SI, et al. A freshwater radiation of diplonemids. Environ Microbiol. 2020;22:4658–68.
23. Lepere C, Masquelier S, Mangot JF, Debroas D, Domaizon I. Vertical structure of small eukaryotes in three lakes that differ by their trophic status: a quantitative approach. ISME J. 2010;4:1509–19.
24. Mukherjee I, Hodoki Y, Okazaki Y, Fujinaga S, Ohbayashi K, Nakano SI. Widespread dominance of kinetoplastids and unexpected presence of diplonemids in deep freshwater lakes. Front Microbiol. 2019;10:2375.
25. Lepère C, Domaizon I, Hugoni M, Vellet A, Debroas D. Diversity and dynamics of active small microbial eukaryotes in the anoxic zone of a freshwater meromictic lake (Pavin, France). Front Microbiol. 2016;7:171591.
26. Monjot A, Bronner G, Courtine D, Cruaud C, Da Silva C, Aury J, Gavory F, Moné A, Vellet A, Wawrzyniak I. Functional diversity of microbial eukaryotes in a meromictic lake: coupling between metatranscriptomic and a trait-based approach. Environ Microbiol. 2023;25:3406–22.
27. Oikonomou A, Pachiadaki M, Stoeck T. Protistan grazing in a meromictic freshwater lake with anoxic bottom water. FEMS Microbiol Ecol. 2014;87:691–703.
28. Šimek K, Grujčić V, Hahn MW, Horňák K, Jezberová J, Kasalický V, Nedoma J, Salcher MM, Shabarova T. Bacterial prey food characteristics modulate community growth response of freshwater bacterivorous flagellates. Limnol Oceanogr. 2018;63:484–502.
29. Moreira D, Lopez-Garcia P. Time series are critical to understand microbial plankton diversity and ecology. Mol Ecol. 2019;28:920–2.
30. Simek K, Nedoma J, Znachor P, Kasalický V, Jezbera J, Hornňák K, Sed'a J. A finely tuned symphony of factors modulates the microbial food web of a freshwater reservoir in spring. Limnol Oceanogr. 2014;59:1477–92.
31. Kavagutti VS, Bulzu PA, Chiriac CM, Salcher MM, Mukherjee I, Shabarova T, Grujcic V, Mehrshad M, Kasalicky V, Andrei AS, et al. High-resolution metagenomic reconstruction of the freshwater spring bloom. Microbiome. 2023;11:15.
32. Shabarova T, Salcher MM, Porcal P, Znachor P, Nedoma J, Grossart HP, Seda J, Hejzlar J, Simek K. Recovery of freshwater microbial communities after extreme rain events is mediated by cyclic succession. Nat Microbiol. 2021;6:479–88.
33. Sommer U, Gliwicz ZM, Lampert W, Duncan A. The PEG-model of seasonal succession of planktonic events in fresh waters. Arch Hydrobiol. 1986;106:433–71.
34. Sommer U, Adrian R, Domis LDS, Elser JJ, Gaedke U, Ibelings B, Jeppesen E, Lürling M, Molinero JC, Mooij WM, et al. Beyond the Plankton Ecology Group (PEG) model: mechanisms driving plankton succession. Annu Rev Ecol Evol Syst. 2012;43:429–48.
35. Park H, Shabarova T, Salcher MM, Kosova L, Rychtecky P, Mukherjee I, Simek K, Porcal P, Seda J, Znachor P, Kasalicky V. In the right place, at the right time: the integration of bacteria into the Plankton Ecology Group model. Microbiome. 2023;11:112.
36. Zeder M, Peter S, Shabarova T, Pernthaler J. A small population of planktonic *Flavobacteria* with disproportionally high growth during the spring phytoplankton bloom in a prealpine lake. Environ Microbiol. 2009;11:2676–86.
37. Eckert EM, Salcher MM, Posch T, Eugster B, Pernthaler J. Rapid successions affect microbial N-acetyl-glucosamine uptake patterns during a lacustrine spring phytoplankton bloom. Environ Microbiol. 2012;14:794–806.
38. Neuenschwander SM, Ghai R, Pernthaler J, Salcher MM. Microdiversification in genome-streamlined ubiquitous freshwater Actinobacteria. ISME J. 2018;12:185–98.
39. Piwosz K, Mukherjee I, Salcher MM, Grujcic V, Simek K. CARD-FISH in the sequencing era: opening a new universe of protistan ecology. Front Microbiol. 2021;12:640066.
40. Grujcic V, Nuy JK, Salcher MM, Shabarova T, Kasalicky V, Boenigk J, Jensen M, Simek K. Cryptophyta as major bacterivores in freshwater summer plankton. ISME J. 2018;12:1668–81.
41. Simek K, Mukherjee I, Nedoma J, de Paula CCP, Jezberova J, Sirova D, Vrba J. CARD-FISH and prey tracer techniques reveal the role of overlooked flagellate groups as major bacterivores in freshwater hypertrophic shallow lakes. Environ Microbiol. 2022;24:4256–73.
42. Simek K, Mukherjee I, Szoke-Nagy T, Haber M, Salcher MM, Ghai R. Cryptic and ubiquitous aplastidic cryptophytes are key freshwater flagellated bacterivores. ISME J. 2023;17:84–94.
43. Znachor P, Nedoma J, Hejzlar J, Seda J, Kopacek J, Boukal D, Mrkvicka T. Multiple long-term trends and trend reversals dominate environmental conditions in a man-made freshwater reservoir. Sci Total Environ. 2018;624:24–33.
44. Sherr EB, Sherr BF. Protistan grazing rates via uptake of fluorescently labeied prey. In: Handbook of methods in aquatic microbial ecology. CRC Press; 2018, pp. 695–701.
45. Brussaard CP. Optimization of procedures for counting viruses by flow cytometry. Appl Environ Microbiol. 2004;70:1506–13.
46. Lund JWG, Kipling C, Le Cren E. The inverted microscope method of estimating algal numbers and the statistical basis of estimations by counting. Hydrobiologia. 1958;11:143–70.
47. Hillebrand H, Dürselen C-D, Kirschtel D, Pollingher U, Zohary T. Biovolume calculation for pelagic and benthic microalgae. J Phycol. 1999;35:403–24.
48. McCauley E. The estimation of the abundance and biomass of zooplankton in samples. In *A manual on methods for the assessment of secondary productivity in fresh waters* 1984.
49. Koste W. Rotatoria. Die Rädertiere Mitteleuropas, begründet von Max Voigt. Überordnung Monogononta. Gebrüder Borntraeger, Berlin, Stuttgart. I. Text (673 pp) u II Tafelbd; 1978.
50. Parada AE, Needham DM, Fuhrman JA. Every base matters: assessing small subunit rRNA primers for marine microbiomes with mock communities, time series and global field samples. Environ Microbiol. 2016;18:1403–14.
51. Martin M. Cutadapt removes adapter sequences from high-throughput sequencing reads. EMBnet J. 2011;17:10–2.
52. Callahan BJ, McMurdie PJ, Rosen MJ, Han AW, Johnson AJ, Holmes SP. DADA2: high-resolution sample inference from Illumina amplicon data. Nat Methods. 2016;13:581–3.
53. Quast C, Pruesse E, Yilmaz P, Gerken J, Schweer T, Yarza P, Peplies J, Glockner FO. The SILVA ribosomal RNA gene database project: improved data processing and web-based tools. Nucleic Acids Res. 2013;41:D590-596.
54. Yilmaz P, Parfrey LW, Yarza P, Gerken J, Pruesse E, Quast C, Schweer T, Peplies J, Ludwig W, Glockner FO. The SILVA and "All-species Living Tree Project (LTP)" taxonomic frameworks. Nucleic Acids Res. 2014;42:D643-648.
55. Guillou L, Bachar D, Audic S, Bass D, Berney C, Bittner L, Boutte C, Burgaud G, de Vargas C, Decelle J, et al. The Protist Ribosomal Reference database (PR2): a catalog of unicellular eukaryote small sub-unit rRNA sequences with curated taxonomy. Nucleic Acids Res. 2013;41:D597-604.
56. Dixon P. VEGAN, a package of R functions for community ecology. J Veg Sci. 2003;14:927–30.
57. Hu A, Ju F, Hou L, Li J, Yang X, Wang H, Mulla SI, Sun Q, Burgmann H, Yu CP. Strong impact of anthropogenic contamination on the co-occurrence patterns of a riverine microbial community. Environ Microbiol. 2017;19:4993–5009.
58. Bastian M, Heymann S, Jacomy M. Gephi: an open source software for exploring and manipulating networks. In: Proceedings of the international AAAI conference on web and social media. 2009, pp. 361–362.
59. Pruesse E, Peplies J, Glockner FO. SINA: accurate high-throughput multiple sequence alignment of ribosomal RNA genes. Bioinformatics. 2012;28:1823–9.
60. Ludwig W, Strunk O, Westram R, Richter L, Meier H, Yadhukumar A, Buchner A, Lai T, Steppi S, Jobb G, et al. ARB: a software environment for sequence data. Nucleic Acids Res. 2004;32:1363–71.
61. Pruesse E, Quast C, Knittel K, Fuchs BM, Ludwig W, Peplies J, Glockner FO. SILVA: a comprehensive online resource for quality checked and aligned ribosomal RNA sequence data compatible with ARB. Nucleic Acids Res. 2007;35:7188–96.

62. Stamatakis A, Ludwig T, Meier H. RAxML-III: a fast program for maximum likelihood-based inference of large phylogenetic trees. Bioinformatics. 2005;21:456–63.
63. Yilmaz LS, Parnerkar S, Noguera DR. mathFISH, a web tool that uses thermodynamics-based mathematical models for in silico evaluation of oligonucleotide probes for fluorescence in situ hybridization. Appl Environ Microbiol. 2011;77:1118–22.
64. Sherr BF, Sherr EB, Fallon RD. Use of monodispersed, fluorescently labeled bacteria to estimate in situ protozoan bacterivory. Appl Environ Microbiol. 1987;53:958–65.
65. Šimek K, Grujčić V, Nedoma J, Jezberová J, Šorf M, Matoušů A, Pechar L, Posch T, Bruni EP, Vrba J. Microbial food webs in hypertrophic fishponds: omnivorous ciliate taxa are major protistan bacterivores. Limnol Oceanogr. 2019;64:2295–309.
66. Jezbera J, Horňák K, Šimek K. Food selection by bacterivorous protists: insight from the analysis of the food vacuole content by means of fluorescence in situ hybridization. FEMS Microbiol Ecol. 2005;52:351–63.
67. Posch T, Eugster B, Pomati F, Pernthaler J, Pitsch G, Eckert EM. Network of interactions between ciliates and phytoplankton during spring. Front Microbiol. 2015;6:1289.
68. Risse-Buhl U, Scherwass A, Schlüssel A, Arndt H, Kröwer S, Küsel K. Detachment and motility of surface-associated ciliates at increased flow velocities. Aquat Microb Ecol. 2009;55:209–18.
69. Gómez F, Wang L, Lin S. Morphology and molecular phylogeny of peritrich ciliate epibionts on pelagic diatoms: *Vorticella oceanica* and *Pseudovorticella coscinodisci* sp. Nov. (Ciliophora, Peritrichia). Protist. 2018;169:268–79.
70. Grossart HP, Simon M. Limnetic macroscopic organic aggregates (lake snow): occurrence, characteristics, and microbial dynamics in Lake Constance. Limnol Oceanogr. 1993;38:532–46.
71. Schoenle A, Hohlfeld M, Rosse M, Filz P, Wylezich C, Nitsche F, Arndt H. Global comparison of bicosoecid *Cafeteria*-like flagellates from the deep ocean and surface waters, with reorganization of the family Cafeteriaceae. Eur J Protistol. 2020;73:125665.
72. Andrei AS, Salcher MM, Mehrshad M, Rychtecky P, Znachor P, Ghai R. Niche-directed evolution modulates genome architecture in freshwater Planctomycetes. ISME J. 2019;13:1056–71.
73. Okazaki Y, Fujinaga S, Tanaka A, Kohzu A, Oyagi H, Nakano SI. Ubiquity and quantitative significance of bacterioplankton lineages inhabiting the oxygenated hypolimnion of deep freshwater lakes. ISME J. 2017;11:2279–93.
74. Wiegand S, Jogler M, Jogler C. On the maverick planctomycetes. FEMS Microbiol Rev. 2018;42:739–60.
75. Grossart H-P, Simon M. Significance of limnetic organic aggregates (lake snow) for the sinking flux of particulate organic matter in a large lake. Aquat Microb Ecol. 1998;15:115–25.
76. Salcher MM, Posch T, Pernthaler J. In situ substrate preferences of abundant bacterioplankton populations in a prealpine freshwater lake. ISME J. 2013;7:896–907.
77. van Grinsven S, Sinninghe Damste JS, Harrison J, Villanueva L. Impact of electron acceptor availability on methane-influenced microorganisms in an enrichment culture obtained from a stratified lake. Front Microbiol. 2020;11:715.
78. Piwosz K, Pernthaler J. Enrichment of omnivorous cercozoan nanoflagellates from coastal Baltic Sea waters. PLoS ONE. 2011;6:e24415.
79. Kuhn S, Medlin L, Eller G. Phylogenetic position of the parasitoid nanoflagellate *Pirsonia* inferred from nuclear-encoded small subunit ribosomal DNA and a description of *Pseudopirsonia* n. gen. and *Pseudopirsonia mucosa* (Drebes) comb. nov. Protist. 2004;155:143–56.
80. Molmeret M, Horn M, Wagner M, Santic M, Abu Kwaik Y. Amoebae as training grounds for intracellular bacterial pathogens. Appl Environ Microbiol. 2005;71:20–8.
81. Watanabe K, Nakao R, Fujishima M, Tachibana M, Shimizu T, Watarai M. Ciliate *Paramecium* is a natural reservoir of *Legionella pneumophila*. Sci Rep. 2016;6:24322.
82. Ok JH, Jeong HJ, Lim AS, Lee SY, Kim SJ. Feeding by the heterotrophic nanoflagellate *Katablepharis remigera* on algal prey and its nationwide distribution in Korea. Harmful Algae. 2018;74:30–45.
83. Mukherjee I, Hodoki Y, Nakano S. *Kinetoplastid flagellates* overlooked by universal primers dominate in the oxygenated hypolimnion of Lake Biwa, Japan. FEMS Microbiol Ecol. 2015;91:fiv083.
84. Caron DA. Grazing of attached bacteria by heterotrophic microflagellates. Microb Ecol. 1987;13:203–18.
85. Brate J, Klaveness D, Rygh T, Jakobsen KS, Shalchian-Tabrizi K. Telonemia-specific environmental 18S rDNA PCR reveals unknown diversity and multiple marine-freshwater colonizations. BMC Microbiol. 2010;10:168.
86. Dokulil M, Skolaut C. Succession of phytoplankton in a deep stratifying lake: Mondsee, Austria. Hydrobiologia. 1986;138:9–24.
87. Mangot J-F, Debroas D, Domaizon I. Perkinsozoa, a well-known marine protozoan flagellate parasite group, newly identified in lacustrine systems: a review. Hydrobiologia. 2011;659:37–48.
88. Jobard M, Wawrzyniak I, Bronner G, Marie D, Vellet A, Sime-Ngando T, Debroas D, Lepère C. Freshwater Perkinsea: diversity, ecology and genomic information. J Plankton Res. 2020;42:3–17.
89. Park MG, Yih W, Coats DW. Parasites and phytoplankton, with special emphasis on dinoflagellate infections. J Eukaryot Microbiol. 2004;51:145–55.
90. Morrison DA. Evolution of the Apicomplexa: Where are we now? Trends Parasitol. 2009;25:375–82.
91. Rösel S, Grossart H-P. Contrasting dynamics in activity and community composition of free-living and particle-associated bacteria in spring. Aquat Microb Ecol. 2012;66:169–81.
92. Paver SF, Hayek KR, Gano KA, Fagen JR, Brown CT, Davis-Richardson AG, Crabb DB, Rosario-Passapera R, Giongo A, Triplett EW, Kent AD. Interactions between specific phytoplankton and bacteria affect lake bacterial community succession. Environ Microbiol. 2013;15:2489–504.
93. Kagami M, Gurung TB, Yoshida T, Urabe J. To sink or to be lysed? Contrasting fate of two large phytoplankton species in Lake Biwa. Limnol Oceanogr. 2006;51:2775–86.
94. Müller H, Schlegel A. Responses of three freshwater planktonic ciliates with different feeding modes to cryptophyte and diatom prey. Aquat Microb Ecol. 1999;17:49–60.
95. Liang D, Luo H, Huang C, Ye Z, Sun S, Dong J, Liang M, Lin S, Yang Y. High-throughput sequencing reveals omnivorous and preferential diets of the rotifer *Polyarthra* in situ. Front Microbiol. 2022;13:1048619.
96. Gilbert JJ. Food niches of planktonic rotifers: diversification and implications. Limnol Oceanogr. 2022;67:2218–51.
97. Devetter M, Seďa J. Regulation of rotifer community by predation of *Cyclops vicinus* (Copepoda) in the Římov Reservoir in spring. Int Rev Hydrobiol. 2006;91:101–12.
98. Šorf M, Brandl Z. The rotifer contribution to the diet of *Eudiaptomus gracilis* (GO Sars, 1863) (Copepoda, Calanoida). Crustaceana. 2012;85:1421–9.
99. Kunzmann AJ, Ehret H, Yohannes E, Straile D, Rothhaupt K-O. Calanoid copepod grazing affects plankton size structure and composition in a deep, large lake. J Plankton Res. 2019;41:955–66.
100. Šimek K, Bobková J, Macek M, Nedoma J, Psenner R. Ciliategrazing on picoplankton in a eutrophic reservoir during the summer phytoplankton maximum: a study at the species and community level. Limnol Oceanogr. 1995;40:1077–90.
101. Metfies K, Berzano M, Mayer C, Roosken P, Gualerzi C, Medlin L, Muyzer G. An optimized protocol for the identification of diatoms, flagellated algae and pathogenic protozoa with phylochips. Mol Ecol Notes. 2007;7:925–36.
102. Bochdansky AB, Huang L. Re-evaluation of the EUK516 probe for the domain eukarya results in a suitable probe for the detection of kinetoplastids, an important group of parasitic and free-living flagellates. J Eukaryot Microbiol. 2010;57:229–35.
103. Mangot JF, Lepere C, Bouvier C, Debroas D, Domaizon I. Community structure and dynamics of small eukaryotes targeted by new oligonucleotide probes: new insight into the lacustrine microbial food web. Appl Environ Microbiol. 2009;75:6373–81.

Publisher's Note